Int J Adv Manuf Technol (2014) 74:1709–1718
DOI 10.1007/s00170-014-6087-x

ORIGINAL ARTICLE

Investigation on the thermal effects during nanometric cutting process while using nanoscale diamond tools

Zhen Tong · Yingchun Liang · Xuechun Yang · Xichun Luo

Received: 21 March 2014 / Accepted: 23 June 2014 / Published online: 9 July 2014

Abstract In this paper, large scale molecular dynamics simulations are carried out to investigate the thermal effect on nanometric cutting of copper while using a single tip and a multi-tip nanoscale diamond tool. A new concept of atomistic equivalent temperature is proposed and used to characterize the temperature distribution in the cutting zone. The results show that the cutting heat generated while using a multi-tip tool is larger than that of using a single tip tool. The local temperature is found to be higher at the inner sides of the multi-tip tool cutting edges than the outer sides. Applying centro-symmetry parameters and radius distribution function, the local annealing process and its effect on the integrity of the machined nanostructures are analyzed. It is observed that the local annealing at the machined surface can improve the surface integrity of the machined nanostructures, especially in the multi-tip diamond tool cutting process. There exists a great potential to control the thickness of residual atomic defect layer through an optimal selection of the cutting speed with designed depth of cut.

Keywords Molecular dynamics · Thermal effect · Nanometric cutting · Multi-tip tool · Nanostructure

Z. Tong · X. Luo (✉)
Department of Design, Manufacture & Engineering Management, University of Strathclyde, Glasgow G1 1XQ, UK
e-mail: xichun.luo@strath.ac.uk

Z. Tong · Y. Liang
Center for Precision Engineering, Harbin Institute of Technology, Harbin 150001, China

X. Yang · X. Luo
Innovative Centre for Unit-Based Logistics Engineering & Technology, Hefei University, Hefei 230601, China

1 Introduction

In recent decades, numerous nanofabrication techniques such as optical and electron beam lithography, focused ion beam (FIB) milling, nanoimprinting, femtosecond laser machining, etc. have been developed to fabricate nanostructures. These nanostructures are the building blocks for many emerging high-tech products such as plasmonic lens, bio-sensors, solar cell, and high density magnetic hard disk etc. [1–3]. However, due to the inherent limitations of these fabrication techniques, particularly the inability for scale-up manufacturing of high quality nanodevices, these methods fail to meet the increasing demand in commercializing functional nanostructured devices.

Diamond turning using multi-tip diamond tools has recently been proven to be a promising method for scale-up manufacturing of micro/nano structures on work material surfaces [2, 4–7]. Through ultra precision scratching/turning operations, it is possible to replicate micro/nano structures pre-featured on the tip of a diamond tool onto a target specimen with high formation accuracy. Periodic micro grooves [4, 5], arrays [6], and diffraction gratings [7] have been successfully obtained by several research groups by using multi-tip tools fabricated by FIB (with tool tip dimensions ranging from 15 to 100 μm). Recently, even nano-gratings with pitch of hundreds of nanometers can be generated by this technique while using nanoscale multi-tip diamond tools (with tool tip width of 150 nm) [2].

However, the formation mechanism of theses nanostructures and the influence factors on form accuracy and surface integrity remain unclear. Obtaining nanostructures with great repeatability is still a challenging task when applying this technique. The cutting heat has long been regarded as a significant factor in nanometric cutting process [3, 8]. It will not only accelerate tool wear, but also significantly influence the material removal, elastic/plastic deformation, and local

thermal annealing. A detailed investigation into the thermal effects is therefore, crucial to gain great controllability and repeatability in the nanometric cutting process.

Molecular dynamics (MD) simulations have been effectively used to address some fundamental issues related to nanometric cutting processes [3, 8–12]. Atomistic models have been applied to emulate the material removal process during nanometric cutting of copper. Ye et al. [3] and Pei et al. [8, 9] built single tip cutting tool models to investigate the material removal mechanism and the cutting heat performed at different cutting speeds. Fang et al. [10], Kim et al. [11], and Yan et al. [12] have used the pin-tool MD model to study the AFM-based nano-scratching processes. Moreover, the role of friction and tool wear in nanometric machining of copper using single tip tool has also been reported [3, 11, 13]. These studies have made significant contributions towards the understanding of the mechanism of diamond turning of copper. However, no experiments or theoretical models have been developed, for nanometric cutting, to study the thermal effect on nanostructure fabrication process while using nanoscale multi-tip diamond tools.

In this paper, atomistic nanometric cutting models are built and conducted to study the thermal effects during the nanometric cutting of copper. In order to benchmark the unique characteristics while using a multi-tip tool, a detailed comparison between the single tip and multi-tip tool cuttings have been carried out in terms of temperature distribution and the integrity of the machined surface.

2 Computational method and the modeling parameters

2.1 Geometric models

To avoid the size effect caused by the period boundary condition [9], large scale nanometric cutting models with free boundary condition in all directions were built for single tip as well as for multi-tip tool cuttings (as shown in Fig. 1). The geometry of the multi-tip cutting tools is shown in Fig. 1a and 1b. The tool tip width is 15a (a=3.567 Å) with the tool rake angle α being 0° and the tool clearance angle β being 12°. To save computational time, a double-tip diamond tool with a pitch of 10a was employed to represent a multi-tip tool. All of the tools were built as deformable bodies with round cutting edges (edge radius of 5a). Copper is chosen as workpiece because of its high machinability for diamond turning, particularly suitable for fabrication of precision drums used in roll-to-roll manufacturing [5]. The workpiece model has a dimension of $50a_0 \times 80a_0 \times 40a_0$ (a_0=3.615 Å). The three orientations of the workpiece are [1 0 0], [0 1 0], and [0 0 1] in the X, Y, and Z directions, respectively.

2.2 Potential functions

There are three types of atomic interactions in the MD simulation. For the Cu–Cu interaction, the embedded atom method (EAM) potential proposed by Foiles et al. [14] was used since it has been successfully used in description of metal materials [3, 9, 15]. The total energy E of the atomistic system comprises summation over the atomistic aggregate of the individual embedding energy F^i of atom i and pair potential ϕ_{ij} between atom i and its neighboring atom j, as shown in the following equation:

$$E = \sum_i F^i\left(\sum_{j\neq i}^{n} \rho^i\left(r^{ij}\right)\right) + \frac{1}{2}\sum_{ij,i\neq j} \phi_{ij}\left(r^{ij}\right) \tag{1}$$

where the lower case Latin superscripts i and j refer to different atoms, r^{ij} is the distance between the atoms i and j, and $\rho^i(r^{ij})$ is the electron density of the atom i contributed by atom j.

For C-C atoms, we adopted the Tersoff potential [16] and computed as follows:

$$V_{ij} = f_C\left(r_{ij}\right)\left[f_R\left(r_{ij}\right) + b_{ij} f_A\left(r_{ij}\right)\right] \tag{2}$$

$$f_C(r) = \begin{cases} 1 : r < R-D \\ \frac{1}{2} - \frac{1}{2}\sin\left(\frac{\pi}{2}\frac{r-R}{D}\right) : R-D < r < R+D \\ 0 : r > R+D \end{cases} \tag{3}$$

$$f_R(r) = A\exp(-\lambda_1 r) \tag{4}$$

$$f_A(r) = -B\exp(-\lambda_2 r) \tag{5}$$

$$b_{ij} = \left(1 + \beta^n \zeta_{ij}^n\right)^{-\frac{1}{2n}} \tag{6}$$

$$\zeta_{ij} = \sum_{k\neq i,j} f_C(r_{ik}) g\left(\theta_{ijk}\right) \exp\left[{\lambda_3}^m \left(r_{ij} - r_{ik}\right)^m\right] \tag{7}$$

$$g\left(\theta_{ijk}\right) = r_{ijk}\left(1 + \frac{c^2}{d^2} - \frac{c^2}{\left[d^2 + \left(cos\theta - \cos\theta_0\right)^2\right]}\right) \tag{8}$$

where V_{ij} is the bond energy of all the atomic bonds, i, j, and k label the atoms of the system, r_{ij} is the length of the ij bond, b_{ij} is the bond order term, θ_{ijk} is the bond angle between the bonds ij and ik, f_R is a two-body term and f_A includes the three-body interactions. f_C merely represents a smooth cutoff function to limit the range of the potential, and ζ_{ij} counts the number of other bonds to atom i besides the ij bond.

Morse potential function was selected to describe the interaction between Cu-C, which has been widely used in MD simulations of nanometric cutting of Cu [12]. A cohesion

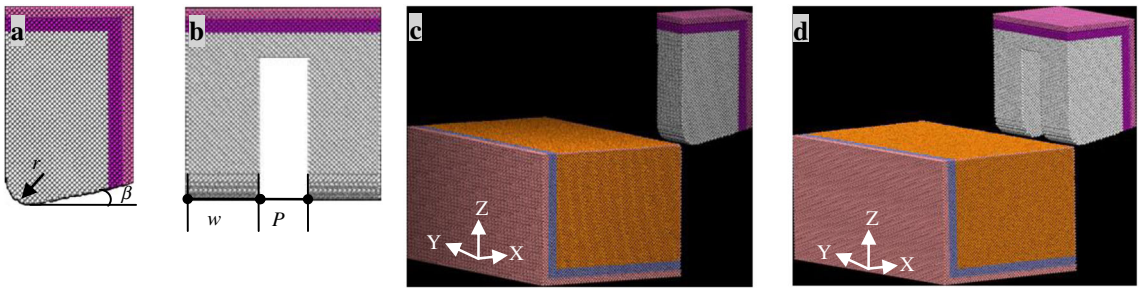

Fig. 1 MD models for nanometric cutting simulation. **a** Side view of cutting tool. **b** Front view of multi-tip cutting tool. **c** Single tip tool cutting model. d Multi-tip tool cutting model

energy D of 0.087 eV, elastic modulus α of 5.14 $Å^{-1}$, and r_0 of 2.05 Å are specified in the present study.

2.3 MD simulation

MD simulations were implemented by using an open source code—LAMMPS [17] compiled on a high performance computing (HPC) clusters using 24 cores. Before cutting, 85,000 computing time steps were carried out to freely relax the system to 293 K. During cutting and the thermal annealing processes, the systems were controlled by NVE ensemble and the thermostat atoms were keeping at a constant temperature of 293 K through using the velocity scaling method to perform the heat dissipation [8, 12]. The other computational parameters used in the MD simulations were summarized in Table 1 for reference.

Figure 2 shows the simulation procedure of the nanometric cutting and the traces of the tool. The cutting tools were applied along the [−1 0 0] direction on the (0 0 1) surface of the copper workpiece. Single tip tool scratched the work surface along the line O_1C_1 for the first cutting pass (as shown in Fig. 2a). Then the tool was moved to point O_2 to scratch again to produce the second nano-groove along the line O_2C_2 with same depth of cut (as shown in Fig. 2b). For multi-tip tool cutting, only a single pass was taken along line OC with the same cutting distance as shown in Fig. 2c. In this case, two nano-grooves were formed at the same time by a single pass. In order to fully reveal the local thermal elastic/plastic recovery of materials during the nanostructure generation processes, after the cutting, all of the models were allowed to relax for 50,000 time steps (50 ps) by holding the tool in the fixed loaded position.

3 Results and discussion

3.1 Temperature distribution

Cutting heat has been regarded as one of the key factors to influence the quality of the generated nanostructures as well as the tool life in nanometric cutting process. According to the law of equipartition of energy, the representative temperature of a group of atoms can be calculated from the total atomic kinetic energies of the group. A new concept of atomistic equivalent temperature T_i, which is calculated from the statistical average temperature of neighbor atoms around the atom i, is proposed in order to more accurately characterize the variation of temperature during the nanometric cutting process. As the nature of the temperature is statistical, the accuracy of the temperature calculated significantly depends on the cutoff distance used. In general, the larger the cutoff distance, the lower the calculated temperature. In this paper, a critical radius $r_0=4a_0$ was employed to select the neighbor atoms in order to reflect the thermal feature of the short-range structure of copper lattice during nanometric cutting

Table 1 Workpiece and simulation parameters

	Single tip with multi-pass	Multi-tip with single pass
Workpiece materials	Copper	Copper
Workpiece dimensions	$50a_0\times80a_0\times40a_0$ (a_0=3.615 Å)	$50a_0\times80a_0\times40a_0$ (a_0=3.615 Å)
Number of atoms	760, 355	894, 870
Time step	1 fs	1 fs
Initial temperature	293 K	293 K
Depth of cut	1 nm	1 nm
Cutting speed	200 m/s	100 m/s, 150 m/s, 200 m/s, 300 m/s

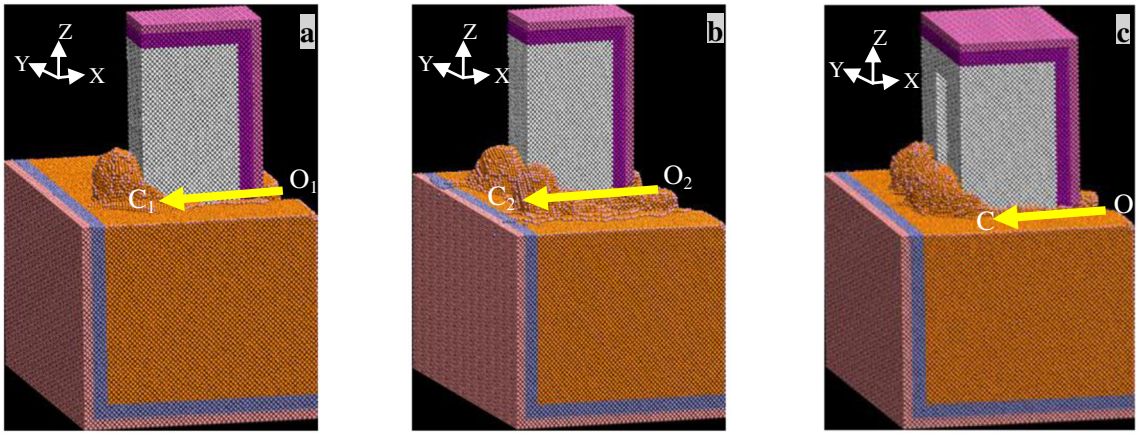

Fig. 2 Schematic of the nanometric cutting traces. **a** Single tip tool cutting (1st cutting pass). **b** Single tip tool cutting (2nd cutting pass). **c** Multi-tip cutting with single pass

processes. The translation between the atomic kinetic energy and the statistical temperature are computed using the following equation:

$$\frac{1}{2}\sum_{j=1}^{n} m_j v_j^2 = \frac{3}{2} n k_B T_i \tag{9}$$

where n is the number of atoms within the radius r_0, m_j and v_j represent the mass and instantaneous velocity, respectively, and k_B is the Boltzmann constant.

The calculated results showed that at initial cutting state, the cutting temperature rapidly increased until it reached a stable value at a cutting distance of 15 nm. Figure 3 shows the detailed temperature distributions of the single tip and multi-tip cutting tools at a cutting distance of 17 nm. Atoms are colored according to their atomistic equivalent temperature. For all the tool models presented here, the highest temperatures were found at the tool cutting edges. For the single tip tool cutting, the atoms with equivalent temperature around 510 K were distributed uniformly around both sides of the tool cutting edges; while for the multi-tip tool cutting, a local temperature of 610 K was found at the inner sides of the tool tips which is higher than other sides. Unlike the single tip tool nanometric cutting where the nano-grooves were generated separately, the two nano-grooves were formed at the same time during multi-tip tool cutting. This will result in a large compression between the inner sides of the tool tips and the workpiece, and thus leading to a high local temperature. Since the high cutting heat is very closely associated with the tool wear, the result indicates that the inner sides' cutting edges of a multi-tip tool are more likely to wear prior to other cutting edges.

Figure 4 shows the cross-sectional view of the atomistic equivalent temperature distribution for the single tip tool and the multi-tip tool cuttings. For better visualization, the white dotted lines are used as the boundaries between the low and high temperature zones (>550 K). It is observed that in all simulations, the temperature in shear zone is around 650 K, but the highest temperature found in the cutting chips is about 900 K. Unlike traditional metal cutting in this study the diamond tool material is significantly harder than the work-piece material i.e., copper. It is a common knowledge that when the cutting tool material is significantly harder than the substrate, the plastic deformation of the softer work material will be the main heat source [18]. In our MD model, the energy transfer between copper and diamond is described by the selected potential functions. At the interface of the diamond tool and copper substrate, there is an atomic layer (with

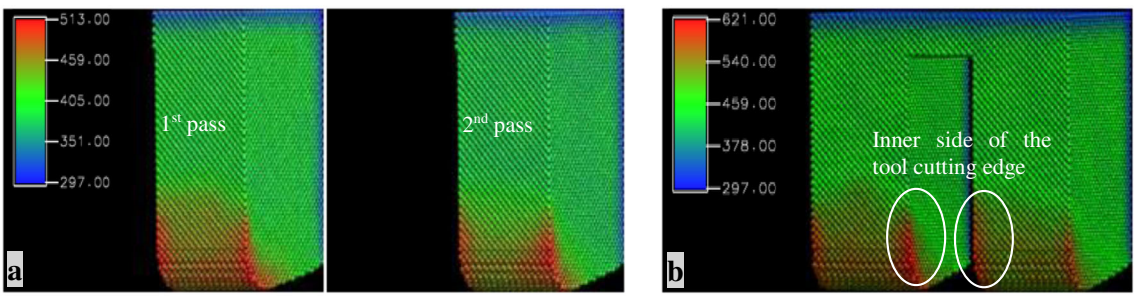

Fig. 3 The temperature distribution of tool tips at a cutting distance of 17 nm. **a** Single tip tool (1st pass and 2nd pass). **b** Multi-tip tool

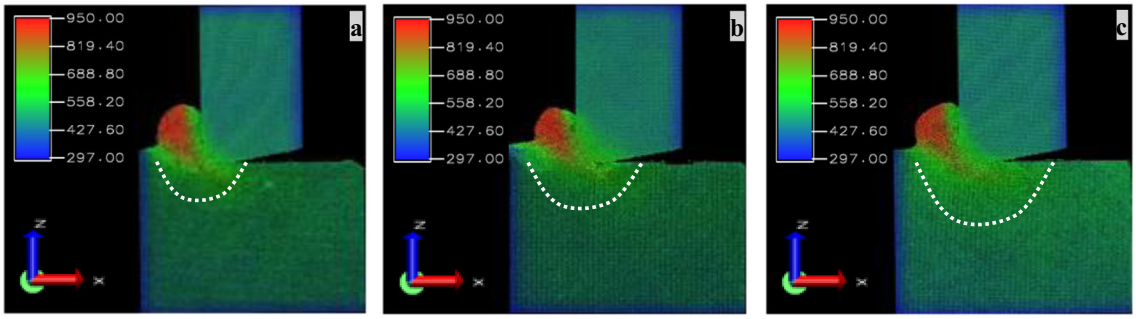

Fig. 4 The cross-sectional views of the temperature distribution at a depth of cut of 17 nm. **a** Single tip tool cutting (1st cutting pass). **b** Single tip tool cutting (2nd cutting pass). **c** Multi-tip tool cutting with single pass

a thickness of several atoms) to transmit the energy between C and Cu atoms. Copper and the diamond materials both have high thermal conductivity. However, the thermal conductivity of the natural diamond was measured to be about 22 W/(cm·K) which is five times more than copper. As a result, a large temperature gradient towards the cutting tool was observed in Fig. 4. Moreover, the large diamond cutting tool model built in the present study also help to release the cutting heat at tool cutting edge. Therefore, the diamond cutting tool would have lower temperature than the copper substrate. The highest cutting temperature was found in the cutting chips.

Nevertheless, it can be seen that the range of high temperature region (>550 K) when using the multi-tip tool is apparently larger than that of using the single tip tool. In order to further quantify the difference in cutting heat when different kinds of tool were used, detailed analysis has been done by comparing the number of atoms in different temperature ranges. For a better comparison, only the workpiece atoms within the cutting zone (z coordination larger than $20a_0$) were taken into account and the numbers of atoms in different temperature ranges were normalized by the total number of atoms selected (as shown in Fig. 5). It was found that the proportion of atoms with atomistic equivalent temperature T_i larger than 500 K in the multi-tip tool case was 8.01 %, which was more than twice larger than that of the single tip tool cutting (being 3.3 %). This result well confirm that the cutting heat generated while using the multi-tip tool was much higher than the cutting heat produced during both the first and the second pass of the single tip tool cutting.

3.2 Thermal annealing at machined surface

It has been widely accepted that re-crystallization happens during local annealing process, not only in ductile metallic materials [3] but also in brittle materials such as silicon [19] and diamond [20]. In macro machining practice, after the tool has left the machined region, there is a macroscopic time (~ms) for the machined surface to relax [3]. And by that time, atomic defects and dislocations under the subsurface might be able to get annealed partly. In nanometric cutting, the thermal effects happen in such a short timescale. To accurately detect and measure the temperature distribution, it requires a thermal measurement system with extremely short response time and high resolution. However, the spectral wavelength of sensors used in most current commercial infra-red thermography are ranging from 0.8 to 14 μm with the response time ranging from 2 to 120 ms. It is therefore very difficult to detect and monitor the cutting heat accurately by current temperature measurement systems. On the other hand, MD simulation provides an effective way to solve this problem by allowing the atomistic insight into the material thermal behavior during nanometric cutting processes.

In the present work, in order to well simulate the relaxation process and investigate the thermal effects when different kinds of tools were used, time relaxations of the machined work material were performed for both the single tip and multi-tip tool cuttings. It has been found through trial simulations that a period of 50 ps relaxation process was enough for the present system to cool down to 293 K. For the

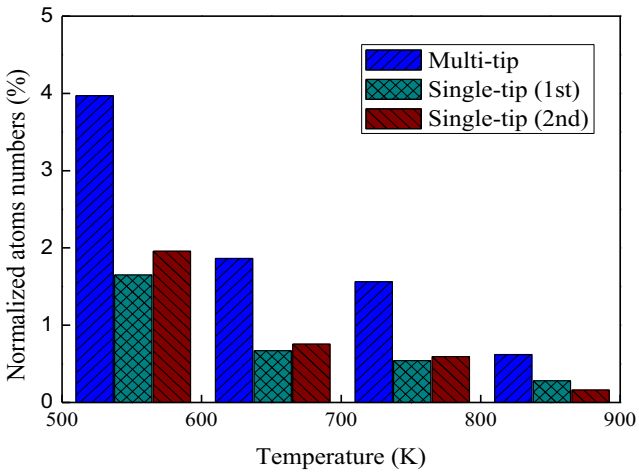

Fig. 5 The proportion of atoms numbers in different temperature ranges

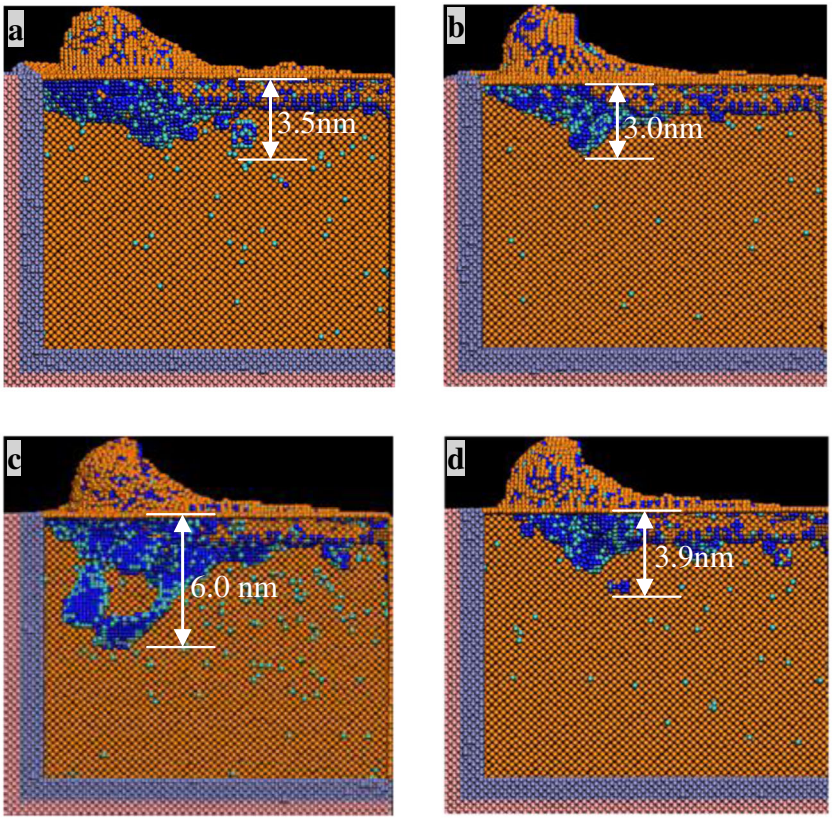

Fig. 6 The cross-sectional views of atomic defects distributions at the machined area after the relaxation for 0 and 50 ps. *Cyan* and *blue atoms* represent particle dislocation and stacking fault, respectively. **a** Single tip tool 2nd cutting pass (0 ps). **b** Single tip tool 2nd cutting pass (50 ps). **c** Multi-tip tool cutting (0 ps). **d** Multi-tip tool cutting (50 ps)

identification of the damages formed during the cutting process, centro-symmetry parameter (CSP) was employed as it is less sensitive to the temperature increase compared with other methods such as atomic coordinate number and the slip vector [9]. Moreover, radial distribution function (RDF) [21] was further employed to identify the changes in the lattice structure during the relaxation process.

Figure 6 shows the cross-sectional views of the defect zones at 0 and 50 ps. For better comparison, only the atoms in the defect zone were selected for analysis and the atoms in the defect-free zone were removed from the visualizations [22]. It can be seen that before the relaxation, there are large numbers of dislocations and atomic defects beneath the tool tip (Fig. 6a, c). The depth of the subsurface atomic defect layer in the multi-tip tool cutting is about ~6 nm which is nearly twice of the single tip tool cutting (being ~3.5 nm). However, as shown in Fig. 6b, most of atomic defects and dislocations in the machined area are annealed after 50 ps for the single tip tool cutting. For multi-tip tool cutting, the atomic defects and dislocations are also remarkably annealed after the relaxation

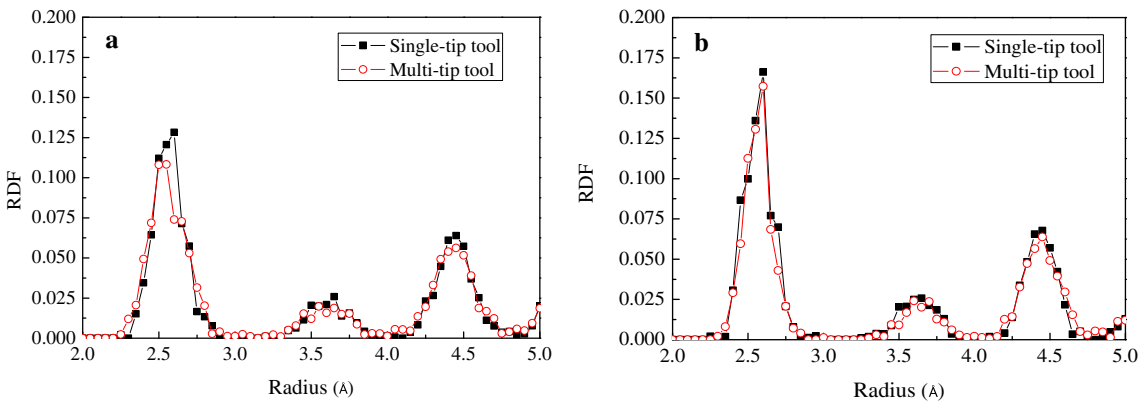

Fig. 7 Radial distribution function (*RDF*) of machined nanostructures. **a** Before relaxation (0 ps). **b** After 50 ps relaxation

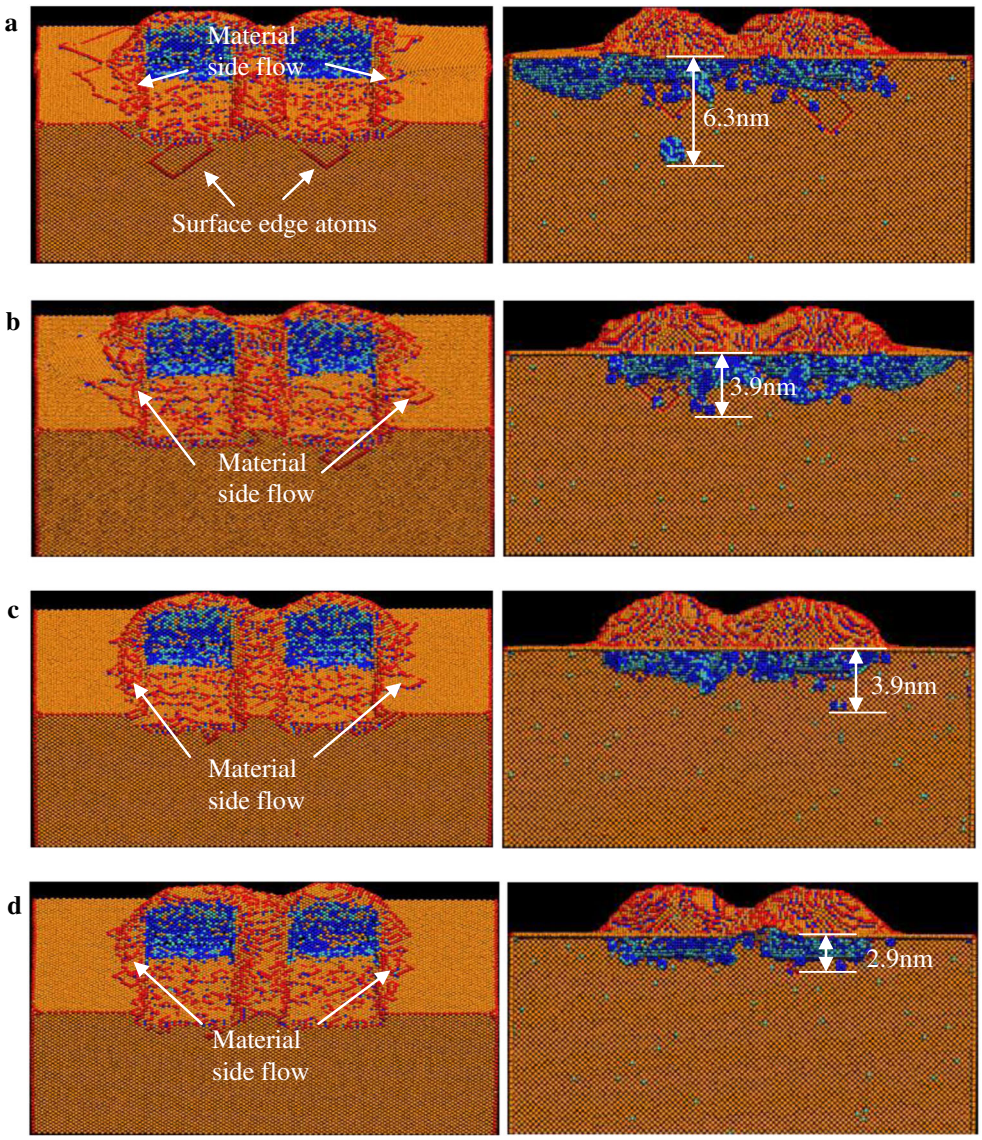

Fig. 8 The nano-grooves and inside views of atomic defects distribution after 50 ps relaxation when using different cutting speeds. *Cyan*, *blue*, and *red* atoms represent particle dislocation, stacking fault, and surface edge atoms, respectively. **a** 100 m/s. **b** 150 m/s. **c** 200 m/s. **d** 300 m/s

process (as shown in Fig. 6d), leaving behind an almost dislocation-free machined workpiece.

In order to further identify the lattice integrity of the machined structure, the radial distribution functions (RDF) of the machined nanostructures were calculated before and after the relaxation process. As shown in Fig. 7a, before relaxation, the RDF value of the first and the third peak for the nanostructure machined by the multi-tip tool are slightly smaller than those of the nanostructure created by using the single tip tool, which indicates that the atoms are in a higher disorder in the case of multi-tip tool cutting; however, after the relaxation process, there is an increase of the first peak value of RDF for both the single tip and multi-tip tool cutting, and the two RDF curves have nearly the same shape (as shown in Fig. 7b). This result is in good agreement with the CSP result and indicates that local re-crystallization takes place on the machined surface.

Nevertheless, it is noted that, the local re-crystallization observed in multi-tip tool cutting is more noticeable than the single tip tool cutting. Although the depth of the atomic defect layer before relaxation when using the multi-tip tool was much larger than that of using the single tip tool, most of the defects were annealed and left almost an ideal FCC lattice structure after the relaxation process. As evident from Fig. 6b, d, the depths of the residual atomic defect layer are 3.0 and 3.9 nm for the single tip and multi-tip tool cuttings, respectively. The cutting heat produced during the nanometric cutting process provides the thermal energy for the defects to get annealed [3]. Therefore, the thermal annealing plays a significant role in obtaining high quality nanostructures

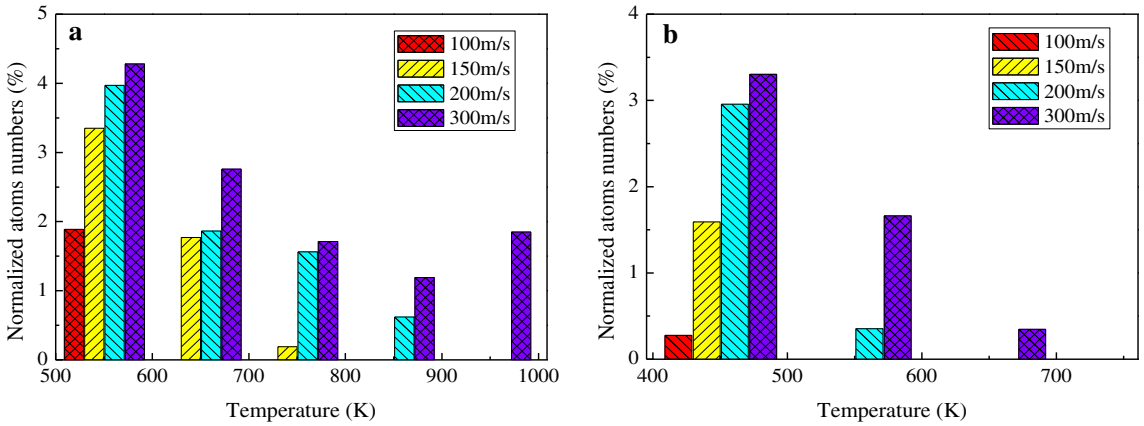

Fig. 9 The proportion of atom numbers in different temperature ranges under different cutting speeds. **a** Temperature of workpieces. **b** Temperature of diamond tools

during the nanometric cutting process, especially when using a multi-tip tool.

3.3 Effect of cutting speed

In metal cutting process, the cutting zone temperature significantly depends on the cutting speed. In order to investigate the thermal effect under different cutting speeds, simulations of nanometric cutting process by using multi-tip tools were performed over a wide range of cutting speed (100, 150, 200, and 300 m/s) with depth of cut of 1 nm.

The nano-grooves and inside views of atomic defects distribution after 50 ps relaxation are shown in Fig. 8. For the case of cutting speed being 100 m/s, there were large numbers of surface edge atoms left (red color) after the relaxation process (Fig. 8a). Because the surface edge atoms also reflects the slip plan of dislocations inside the workpiece, to some extent, the density and distribution of these edge atoms are able to indicate the range and slip plans of material plastic flow [22]. It is found that with the increase of the cutting speed, especially when the cutting speed is higher than 200 m/s, the number of surface edge atoms and the range of material side flow are remarkably decreased. The nano-grooves machined by using a cutting speed of 300 m/s have the best surface integrity (as shown in Fig. 8b–d). Moreover, the range and depth of residual atomic defect layer after annealing were found to be significantly decreased with the cutting speed. The depth of residual damaged layer being 2.9 nm under the cutting speed of 300 m/s is much smaller than that of 6.3 nm for the case of the cutting speed at 100 m/s; while, the depth of residual damaged layer for the cases of 150 m/s and 200 m/s are the same (being 3.9 nm). Under all of the above cutting conditions, no extra thermo-induced damage was found after a cutting distance of 18 nm. The result indicates the great potential to control the thickness of residual atomic defect layer through selection of optimal cutting speed under the adopted depth of cut when using nanoscale multi-tip diamond tools.

To achieve better understanding of the effect of cutting speed on the cutting heat produced during the nanometric cutting process, the proportions of atoms with atomistic temperature that is larger than 400 K are calculated and shown in Fig. 9. On one hand, the cutting heat increases with the increase of the operational cutting speed. As shown in Fig. 9a, the proportion of atoms at each temperature range increase with the increase of the cutting speed. However, the existence of workpiece atoms with the equivalent atomistic temperature that is larger than 600 K only appears when the cutting speed is equal or larger than 150 m/s. This important result explains well the variation of surface integrity and the depth of residual subsurface atomic defect layer under different cutting speeds which has been discussed above. When the cutting speed is high enough, the cutting heat generated at the high cutting speed would provide enough thermal energy for annealing the atomic defects and facilitating the nanostructure formation process as the dislocations movement and diffusional creep are more easy to activate at a relatively high temperature [23]. The higher the cutting speed, the higher the local cutting heat generated, and thus the less the numbers of residual atomic defects left.

On the other hand, the high cutting heat produced at high cutting speed will result in the initialization of the tool wear at the cutting edge and decrease the tool life [24, 25]. Figure 9b shows the proportions of the diamond tool atoms in different temperature ranges. It is found that the tool atoms with the equivalent atomistic temperature that is larger than 500 K only appears when the cutting speed is higher than 150 m/s. Although the high cutting heat produced at high cutting speed would provide enough thermal energy for annealing the atomic defects [3], to some extent, the increase of the cutting heat at

the tool cutting edges would in turn soften the C-C bond strength and accelerate the tool wear [26]. In this sense, a high cutting speed is not preferable due to the early-induced tool wear. Moreover, the vibrations and the motional errors induced by the increase of cutting speed would degrade the formation accuracy of the nanostructures and the surface integrity. As a result, it is to be concluded that a balance between the targeted quality of nanostructures and the tool life should be critically considered while choosing the cutting speed for the diamond turning with nanoscale multi-tip tools.

4 Conclusions

The MD simulations presented in this paper reveal the detailed thermal behaviors of work materials and provide a useful theoretical support for determining the cutting speed when performing the nanometric cutting using nanoscale multi-tip diamond tools. The conclusions can be drawn as follows:

(1) The atomistic equivalent temperature provides a new effective way to characterize local temperature distribution during nanometric cutting processes. The highest temperature was found in cutting chips. The cutting heat produced during multi-tip tool cutting is found to be larger than the single tip tool cutting.
(2) The local temperature is found to be higher at the inner sides of the nanoscale multi-tip diamond tool cutting edges than that of the outer sides suggesting that the inner sides' cutting edges are more likely to wear prior to other cutting edges.
(3) Local thermal annealing process takes place on the machined area and plays a major role in obtaining high quality nanostructures. When the cutting heat produced during the cutting process is high enough, most of the subsurface atomic defects are able to get annealed during the relaxation process.
(4) High cutting speed can accelerate thermal annealing process observed at the machined area. A balance between the machining quality of nanostructures and the tool life should be critically considered while choosing the cutting speed for nanometric cutting with nanoscale multi-tip tools.

Acknowledgments The authors gratefully acknowledge the financial support from EPSRC (EP/K018345/1), Sino-UK Higher Education Research Partnership for PhD Studies (CPT508), the National Funds for Distinguished Young Scholars (No. 50925521) and Wanjiang Scholar of China. The authors would also like to acknowledge the technical supports from the HPC team at the University of Huddersfield and assess to Huddersfield Queensgate Grid for MD simulations in this study.

References

1. Kong LB, Cheung CF, Jiang XQ, Lee WB, To S, Blunt L, Scott P (2010) Characterization of surface generation of optical microstructures using a pattern and feature parametric analysis method. Precis Eng 34:755–766
2. Sun J, Luo X, Chang W, Ritchie JM, Chien J, Lee A (2012) Fabrication of periodic nanostructures by single-point diamond turning with focused ion beam built tool tips. J Micromech Microeng 22:115014
3. Ye YY, Biswas R, Morris JR, Bastawros A, Chandra A (2003) Molecular dynamics simulation of nanoscale machining of copper. Nanotechnology 14:390–396
4. Adamsa DP, Vasile MJ, Krishnan ASM (2000) Microgrooving and microthreading tools for fabricating curvilinear features. Precis Eng 24:347–356
5. Picard YN, Adams DP, Vasile MJ, Ritchey MB (2003) Focused ion beam-shaped microtools for ultra-precision machining of cylindrical components. Precis Eng 27(1):59–69
6. Ding X, Lim GC, Cheng CK, Butler DL, Shaw KC, Liu K, Fong WS (2008) Fabrication of a micro-size diamond tool using a focused ion beam. J Micromech Microeng 18:075017
7. Xu ZW, Fang FZ, Zhang SJ, Zhang XD, Hu XT, Fu YQ, Li L (2010) Fabrication of micro DOE using micro tools shaped with focused ion beam. Opt Express 18(8):8025–8032
8. Pei QX, Lu C, Lee HP (2007) Large scale molecular dynamics study of nanometric machining of copper. Comput Mater Sci 41(2):177–185
9. Pei QX, Lu C, Lee HP, Zhang YW (2009) Study of materials deformation in nanometric cutting by large-scale molecular dynamics simulations. Nanoscale Res Lett 4:444–451
10. Fang TH, Weng CI (2000) Three-dimensional molecular dynamics analysis of processing using a pin tool on the atomic scale. Nanotechnology 11:148–153
11. Cho MH, Kim SJ, Lim DS, Jang H (2005) Atomic scale stick–slip caused by dislocation nucleation and propagation during scratching of a Cu substrate with a nanoindenter: a molecular dynamics simulation. Wear 259(7–12):1392–1399
12. Yan Y, Sun T, Dong S, Liang Y (2007) Study on effects of the feed on AFM-based nano-scratching process using MD simulation. Comput Mater Sci 40(1):1–5
13. Lin ZC, Huang JC (2008) A study of the estimation method of the cutting force for a conical tool under nanoscale depth of cut by molecular dynamics. Nanotechnology 19:115701
14. Foiles SM, Baskes MI, Daw MS (1986) Embedded-atom-method functions fo the fcc metals Cu, Ag, Au, Ni, Pd, Pt, and their alloys. Phys Rev B 33(12):7983–7991
15. Zhu PZ, Hu YZ, Ma TB, Wang H (2010) Study of AFM-based nanometric cutting process using molecular dynamics. Appl Surf Sci 256(23):7160–7165
16. Tersoff J (1988) New empirical approach for the structure and energy of covalent systems. Phys Rev B Condens Matter 37(12):6991–7000
17. Plimpton S (1995) Fast parallel algorithms for short range molecular dynamics. J Comput Phys 117:1–19
18. Norouzifard V, Hamedi M (2014) Experimental determination of the tool–chip thermal contact conductance in machining process. Int J Mach Tools Manuf 84:45–57
19. Nordlund K, Averback RS (1997) Point defect movement and annealing in collision cascades. Phys Rev B 56:2421–2431
20. Kalish R, Reznik A, Prawer S, Saada D, Adler J (1999) Ion-implantation-induced defects in diamond and their annealing: experiment and simulation. Phys Status Solidi 174:83–99
21. <http://isaacs.sourceforge.net/phys/rdfs.html>, g(r) RDF explanation accessed on 21 Nov 2011
22. Tong Z, Liang YC, Jiang XQ, Luo XC (2014) An atomistic investigation on the mechanism of machining nanostructures when using single tip and multi-tip diamond tools. Appl Surf Sci 290:458–465

23. Lu L, Sui ML, Lu K (2000) Superplastic extensibility of nanocrystalline copper at room temperature. Science 287:1463–1466
24. Saglam H, Yaldiz S, Unsacar F (2007) The effect of tool geometry and cutting speed on main cutting force and tool tip temperature. Mater Des 28:101–111
25. Kim SJ, Le D, Lee SW, Song KH, Lee DY (2014) Experiment-based statistical prediction on diamond tool wear in micro grooving Ni-P alloys. Diam Relat Mater 41:6–13
26. Cheng K, Luo X, Ward R, Holt R (2003) Modeling and simulation of the tool wear in nanometric cutting. Wear 255:1427–1432